M&C 2017 - International Conference on Mathematics & Computational Methods Applied to Nuclear Science & Engineering, Jeju, Korea, April 16-20, 2017, on USB (2017)

On-The-Fly Multigroup Weighting in PARTISN

Thomas G. Saller, Randal S. Baker, Jon A. Dahl

CCS-2, Los Alamos National Laboratory, P.O. Box 1663, Los Alamos, NM, 87545
tgsaller@lanl.gov

Abstract - *The choice of a weight function in multigroup neutron transport significantly affects the accuracy of the multigroup solution. Weight functions are often selected to reflect the solution to a simplified 0-, 1-, or 2-D problem, so the applicability of these functions to realistic problems can be problematic. We introduce on-the-fly (OTF) weight functions to address this issue. OTF weight functions ideally allow few group cross sections to more accurately represent the true solution of a problem without requiring cross sections for each potential final solution. With OTF weight functions, fine group cross sections are periodically collapsed to a coarse group structure, and the multigroup transport equation is solved on the coarse energy grid. Fine group OTF weight functions are obtained by applying a fit to the latest coarse group fluxes and scaling the original weight functions by this fit. In this paper, we focus on four piecewise linear fits, or prolongations, for mapping the coarse group solution to fine group weight functions. The four OTF prolongations are applied to three LANL coarse group structures (30, 133, and 250 energy groups) and tested with five simple problems. The OTF prolongations typically show an improvement over the standard group collapse method, both in eigenvalue and reaction rates. Although OTF weighting struggled in moderator regions, in nearly every case it improved both the removal and fission rates in fissile regions. Spatial fission rates were similarly improved. While re-collapsing multigroup cross sections on-the-fly is not a new concept, the OTF weighting method presented here is unique in requiring no additional transport sweeps, coarse or fine. Our results show that with OTF weighting we can perform a coarse group transport solve and obtain results similar in accuracy to a fine group solution, using minimal additional calculations.*

I. INTRODUCTION

One of the fundamental assumptions in deterministic neutron transport is the multigroup approximation [1, 2]. Neutron energies in practical problems may range over eight orders of magnitude, and over that range neutron cross sections can vary rapidly with respect to the energy variable E. To resolve these rapid variations on an energy grid would require tens of thousands of energy groups. In the multigroup approximation, however, continuous energy cross sections are collapsed to significantly fewer energy groups, often tens or hundreds, by taking a weighted average of the energy-dependent cross sections for a specified energy group structure.

The choice of a weight function greatly impacts the accuracy of the multigroup solution. Weight functions are typically chosen to reflect the solution to a simplified 0-, 1-, or 2-D problem that is "close to" the problem under consideration. The applicability of these weight functions to problems that are multidimensional, heterogeneous, and comprised of many materials can be questionable. Furthermore, weight functions are often problem-specific. If the problem changes, new weight functions must be generated, a potentially time-consuming process. We seek a weight function that properly models a heterogeneous problem without requiring many additional calculations. To do so, we introduce on-the-fly (OTF) weight functions.

OTF weight functions ideally allow few group cross sections to better reflect the fine group solution of a problem without requiring a set of cross sections for each potential final solution. With OTF weight functions, fine group cross sections are periodically collapsed (or condensed) to a coarse group structure, and the multigroup transport equation is solved on the coarse energy grid. Fine group OTF weight functions are obtained by applying a fit to the latest coarse group scalar fluxes and scaling the original weight function by the fit. In this paper, we focus on four piecewise linear (PL) fits, or prolongations, for mapping the coarse group fluxes to the fine group structure.

Because the OTF prolongations are piecewise linear functions, they are incapable of capturing rapid flux variations within a coarse group, such as those caused by resonances. Instead of applying the prolongated fluxes directly, we use them to scale the weight functions provided with the fine group cross sections. In this work, the fine group cross sections and weight functions were generated by NJOY with an array of background cross sections. During run-time, these weight functions are scaled by the OTF prolongations, and the resultant weight function is used to re-collapse (re-condense) the microscopic fine group cross sections. The Bondarenko method [3] is then applied to these coarse group, σ_0-dependent cross sections to obtain the macroscopic cross sections used by the transport solver.

In this paper, the four OTF prolongations are tested with five simple problems (either 1-D or 2-D). 618 group cross sections are generated using the LANL TD-4 weight function [4] with background cross sections (σ_0). The four OTF prolongations and the standard group collapse method are applied to three standard LANL coarse group structures (30, 133, and 250 energy groups) [5]. The 618 group PARTISN solution is used as a reference, and MCNP results are reported for additional comparisons. In almost every case, the OTF results show improvement in both eigenvalue and reaction rates over

the standard condensation method. While a reduction in error is seen with all three coarse group structures, the improvement is more significant with fewer coarse groups. With 133 and 250 coarse groups, all four OTF prolongations perform similarly.

II. BACKGROUND

Using a coarse group calculation to approximate the fine group flux is not a new idea. For example, the generalized energy condensation (GEC) theory [6] uses orthogonal functions to expand the flux within a coarse group in energy. This leads to a series of multigroup equations that can be solved for flux moments that are used to construct an approximate continuous energy angular flux. By choosing orthogonal functions to expand the flux it is possible to decouple the higher order equations from each other, which greatly reduces the computational burden from solving additional multigroup equations. The source for these extra equations depends only on the solution to the zeroth-order equation, which is equivalent to the standard multigroup equation. Unfortunately, this also means that the eigenvalue remains unchanged from the original coarse group solution.

A natural extension to GEC theory is to use the expanded flux to re-collapse the fine group cross sections on-the-fly [7], similar to this work. This allows the coarse group cross sections to better capture the problem of interest, which was shown to produce an improved eigenvalue. Rahnema et al. demonstrated that with a sufficient number of flux moments the coarse group solution can approach the best-case solution, one where the cross sections had been collapsed with the true fine group flux. A further improvement [8] introduced a term to account for the angular dependence of the multigroup total cross section. This extra term significantly reduced the error seen with few group solutions, particularly in highly anisotropic test problems.

Though it produces a continuous energy solution with only coarse group calculations, GEC theory can suffer from negative fluxes and unphysical oscillations near group boundaries. The discrete generalized multigroup (DGM) method [9] was developed to address these concerns. The DGM method modifies the GEC theory by applying discrete, rather than continuous, functions to expand the coarse group flux. This produces an expanded flux closer to the fine group flux solution. Furthermore, source updates yield an improved eigenvalue and eliminate all negative fluxes. Combining the DGM method with re-condensation led to results on par with a fine group solution after only a few DGM iterations [10].

Both GEC theory and the DGM method use additional coarse group transport sweeps to obtain estimates of the continuous or fine group fluxes for a problem. The accuracy of these estimates depends on the expansion ordered selected. While these extra equations have a known source and are quick to solve, they still require additional sweeps over space. OTF weight functions, while less accurate, require only simple calculations for each coarse mesh spatial region and no additional transport sweeps. Re-condensation of the multigroup cross sections is performed identically for each method.

The subgroup decomposition (SGD) method [11] is another method for re-collapsing cross sections on-the-fly. Unlike GEC theory and the DGM method, it does not require additional flux moments. Rather, it uses the coarse group fluxes from an iteration to generate the source for a fixed-source fine group problem. This fixed-source problem is solved with a single "decomposition sweep," which provides fine group fluxes that are then used to re-collapse the fine group cross sections for the next coarse group iteration. The primary difference between our method and the SGD method is the decomposition sweep, which replaces the prolongation step in the OTF method.

The SGD method, like GEC theory and the DGM method, invariably produces more accurate solutions than our OTF weighting method. However, it requires an additional fine group sweep per outer iteration. For problems that require many coarse group sweeps per outer iteration, this additional sweep adds only a small computational burden. For problems with few transport sweeps per outer iteration, or many more fine groups than coarse groups, this additional sweep may significantly impact run-time. In many time-dependent simulations, for instance, very few outer iterations are performed per time step. Thus, adding a fine group sweep for every time step could lead to run-times comparable to a standard fine group calculation.

III. MULTIGROUP THEORY

We apply the OTF weighting method to the 1-D, steady-state, multigroup transport equation:

$$\begin{aligned}\mu\frac{\partial}{\partial x}\psi_g(x,\mu)+\Sigma_{t,g}(x)\psi_g(x,\mu)&\\ =\sum_{g'=1}^{G}\int_{-1}^{1}\Sigma_{s,g'\to g}(x,\mu'\to\mu)\psi_{g'}(x,\mu')\,d\mu'&\\ +\frac{1}{k}\sum_{g'=1}^{G}\chi_{g'\to g}(x)\nu\Sigma_{f,g'}(x)\phi_{g'}(x)\ ,&\end{aligned}\tag{1}$$

where $\psi_g(x,\mu)$ is the multigroup neutron angular flux for group g, $\Sigma_g(x)$ is a macroscopic multigroup cross section (t = total, s = scattering, f = fission), $\chi_{g'\to g}(x)$ is the fission transfer matrix, ν is the average number of neutrons produced per fission, k is the multiplication factor, and ϕ_g is the multigroup scalar flux:

$$\phi_g(x)=\int_{-1}^{1}\psi_g(x,\mu)\,d\mu\ .\tag{2}$$

The multigroup cross sections in Eq. (1) are obtained by weighting the continuous energy cross sections with a predetermined weight function, $f(E)$, over an energy group, $\Delta g=[E_{g+1/2},E_{g-1/2}]$, which yields [1, 2]:

$$\Sigma_{t,g}(x)=\frac{\int_{\Delta g}\Sigma_t(x,E)f(E)\,dE}{f_g}\ ,\tag{3a}$$

$$\Sigma_{s,g'\to g}(x,\mu'\to\mu)=\frac{\int_{\Delta g}\int_{\Delta g'}\Sigma_s(x,E'\to E,\mu'\to\mu)f(E')\,dE'\,dE}{f_{g'}}\ ,\tag{3b}$$

and

$$\nu\Sigma_{f,g}(x) = \frac{\int_{\Delta g} \nu\Sigma_f(x,E)\, f(E)\, dE}{f_g} , \tag{3c}$$

where

$$f_g = \int_{\Delta g} f(E)\, dE . \tag{3d}$$

The fission transfer matrix is fission-weighted, rather than flux-weighted:

$$\chi_{g'\to g}(x) = \frac{\int_{\Delta g}\int_{\Delta g'} \chi(x,E'\to E)\,\nu\Sigma_f(x,E')\, f(E')\, dE' dE}{\int_{\Delta g'} \nu\Sigma_f(x,E')\, f(E')\, dE'} . \tag{3e}$$

Clearly, the accuracy of $\psi_g(x,\mu)$ is linked to the accuracy of the weight function, $f(E)$. A poor choice for $f(E)$ will lead to poorly defined multigroup cross sections and an inaccurate angular flux. On the other hand, if $f(E)$ is the true continuous energy scalar flux for the problem (i.e. $f(E)$ is space-dependent, and $f(x,E) = \phi(x,E)$), then Eqs. (1) – (3) are exact (ignoring any potential angular dependence of the multigroup total cross section). We rarely (if ever) have the exact solution when calculating multigroup constants and are instead forced to use an estimate of $\phi(x,E)$.

Typically, multiple group collapses (e.g., from continuous energy to fine group to coarse group) are performed with a different weight function at each stage. For collapsing from the continuous energy cross sections (actually point-wise, with tens of thousands of energy points), a generic spectrum is often used for each isotope. Self-shielding corrections may be applied to this spectrum to better account for multiple isotopes in a single material.

One correction method is to introduce a "background cross section" (σ_0) to approximate the other isotopes in a material. By breaking the macroscopic total cross section of a material into two parts,

$$\Sigma_t(E) = N^m \sigma_t^m(E) + \sum_{n\neq m} N^n \sigma_t^n(E) , \tag{4}$$

we can replace the summation in Eq. (4) with a background cross section:

$$\Sigma_t(E) = N^m \left(\sigma_t^m(E) + \sigma_0^m(E)\right) , \tag{5}$$

where

$$\sigma_0^m(E) = \frac{1}{N^m} \sum_{n\neq m} N^n \sigma_t^n(E) . \tag{6}$$

Including σ_0 adjusts the weight function for each isotope ($f(E) \to f^m(E,\sigma_0)$), producing a set of σ_0-dependent microscopic multigroup cross sections. Once the parameterized multigroup data is obtained, a self-shielding technique, such as the Bondarenko method [3], is used to generate self-shielded macroscopic multigroup cross sections for each problem-dependent material.

Because the microscopic total cross sections $\sigma_t^n(E)$ in Eq. (6) may also be self-shielded, an iterative technique is required to converge the background cross sections. Once one obtains self-shielded total cross sections for an initial guess of σ_0^m, updated background cross sections are calculated with Eq. (5), and new total cross sections are obtained. This process is repeated until the change in σ_0^m from one iteration to the next is within a desired tolerance.

Often the fine group data includes fine group weight functions for each isotope and background cross section $\left(f_g^m(\sigma_0)\right)$ so that further group collapses can be performed without any additional calculations. Alternately, coarse group cross sections can be obtained by performing a fine group transport calculation for each material or region and using the flux solution to collapse the fine group cross sections. In reactor physics, this calculation is typically performed for either a pin cell or a fuel assembly with self-shielded cross sections. Because reflecting boundary conditions are often used, this is referred to as a "lattice calculation."

Performing a group collapse from a fine group structure to a coarser one is similar to condensing the continuous energy cross sections to multigroup. Rather than a weighted integral over energy, we use a weighted summation over energy groups. Given a fine group structure with K groups and a coarse group structure with G groups, Eqs. (3) become:

$$\Sigma_{t,g}(x) = \frac{\sum_{k=h_{g+1/2}}^{h_{g-1/2}} \Sigma_{t,k}(x)\, f_k}{f_g} , \tag{7a}$$

$$\Sigma_{s,g'\to g}(x,\mu'\to\mu) = \frac{\sum_{k=h_{g+1/2}}^{h_{g-1/2}} \sum_{k'=h_{g'+1/2}}^{h_{g'-1/2}} \Sigma_{s,k'\to k}(x,\mu'\to\mu)\, f_{k'}}{f_{g'}} , \tag{7b}$$

$$\nu\Sigma_{f,g}(x) = \frac{\sum_{k=h_{g+1/2}}^{h_{g-1/2}} \nu\Sigma_{f,k}(x)\, f_k}{f_g} , \tag{7c}$$

$$f_g = \sum_{k=h_{g+1/2}}^{h_{g-1/2}} f_k , \tag{7d}$$

and

$$\chi_{g'\to g}(x) = \frac{\sum_{k=h_{g+1/2}}^{h_{g-1/2}} \sum_{k'=h_{g'+1/2}}^{h_{g'-1/2}} \chi_{k'\to k}(x)\,\nu\Sigma_{f,k'}(x)\, f_{k'}}{\sum_{k'=h_{g'+1/2}}^{h_{g'-1/2}} \nu\Sigma_{f,k'}(x)\, f_{k'}} , \tag{7e}$$

where $k = h_{g\pm1/2}$ is the upper (-) or lower (+) fine group in coarse group g.

These methods are far from the only options to obtain multigroup cross sections. The Oak Ridge National Laboratory code CENTRM performs a 1- or 2-D fixed-source calculation with point-wise cross section data [12]. The flux solution is then used to collapse the continuous energy cross sections to multigroup. These calculations can be computationally expensive, particularly because they must be performed at run time for each region of interest. However, the result is more accurate than simpler self-shielding methods because CENTRM explicitly handles heterogeneities and overlapping resonances.

In this work, we use the TD-4 weight function [4] for $f(E)$. The TD-4 weight function consists of four main regions

– a thermal Maxwellian spectrum, a 1/E slowing down region, a fission spectrum, and a fusion peak. Isotope-dependent 618 group cross sections are calculated with the NJOY nuclear data processing system [13] for six background cross section values, ranging from $\sigma_0 = 0.1$ to $\sigma_0 = 10^{10}$ (infinitely dilute).

The fine group cross sections are collapsed to the three LANL coarse group structures by one of two methods. The first is the standard method, which uses the fine group weights from NJOY for each individual isotope to collapse the 618 group cross sections. In the second method, the fine group weight functions from NJOY are periodically scaled by the OTF prolongations. The fine group data is then re-condensed with the adjusted weight functions. Both methods perform group collapses with Eqs. (7); they differ only in the weight function used.

Once the coarse group cross sections are obtained for each isotope, they are mixed with the Bondarenko method. For the Bondarenko method, PARTISN calculates $\sigma^m_{0,g}$ for each isotope m and energy group g, and then interpolates between points in the background cross section grid to obtain self-shielded, group-dependent cross sections $\left(\sigma^m_g(\sigma^m_{0,g})\right)$. The $\sigma^m_{0,g}$ interpolation is performed with the square root of the background cross sections:

$$\sigma^m_g\left(\sigma^i_{0,g}\right) = \frac{\sigma^m_g\left(\sigma^m_{0,g,h}\right) - \sigma^m_g\left(\sigma^m_{0,g,h-1}\right)}{\sqrt{\sigma^m_{0,g,h}} - \sqrt{\sigma^m_{0,g,h-1}}}\left(\sqrt{\sigma^m_{0,g}} - \sqrt{\sigma^m_{0,g,h-1}}\right) + \sigma^m_g\left(\sigma^m_{0,g,h-1}\right), \quad (8)$$

where $\sigma^m_g(\sigma_0)$ is a microscopic cross section for group g and background cross section σ_0, $\sigma^m_{0,g}$ is the calculated background cross section, $\sigma^m_{0,g,h}$ is a point on the background cross section grid, and

$$\sigma^m_{0,g,h-1} \leq \sigma^m_{0,g} \leq \sigma^m_{0,g,h} \, . \quad (9)$$

The choice of square-root interpolation was motivated by the original WIMS lattice code [14]. Modern neutron transport codes use more complicated interpolation schemes. For example, the transport code MPACT [15] uses "Segev" interpolation [16].

IV. ON-THE-FLY WEIGHTING

The OTF weighting method is illustrated in Figure 1 and detailed below.

First, we define a fine group structure with K energy groups and a coarse group structure with G energy groups, where $G < K$. Fine group cross sections and weight functions are obtained from NJOY as a function of isotope (m) and background cross section (σ_0). The fine group weight functions are collapsed to the coarse group structure before being prolongated with one of the OTF methods back onto the fine group structure. The fine group weight functions ($f_{m,k}(\sigma_0)$), cross sections ($\Sigma_{m,k}(\sigma_0)$), and prolongated weight functions $\left(\widehat{f}_{m,k}(\sigma_0)\right)$ are all stored.

Initial coarse group cross sections are obtained by performing a group collapse on the fine group cross sections with the weight functions from NJOY and combining the results with the Bondarenko method. These cross sections $\left(\Sigma^{(0)}_{j,g}\right)$ are

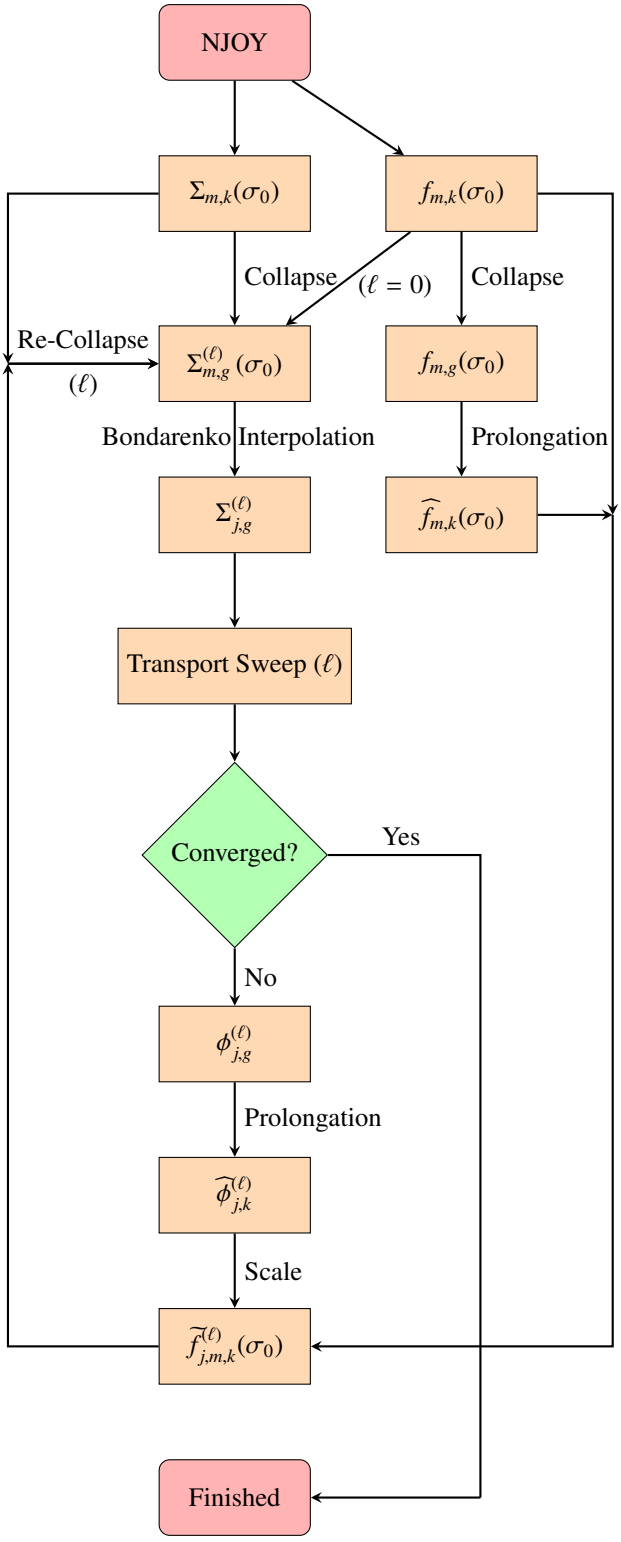

Fig. 1: OTF Weighting Flow Chart

then used in a outer iteration. At the end of an outer iteration (ℓ), coarse group scalar fluxes are calculated for each coarse mesh region (j). These fluxes $\left(\phi_{j,g}^{(\ell)}\right)$ are then prolongated onto the fine group structure with the same OTF method used previously to obtain prolongated fluxes for iteration ℓ $\left(\widehat{\phi}_{j,g}^{(\ell)}\right)$.

Next, the stored fine group weight functions are scaled by a ratio of the current iteration's prolongated fluxes to the stored prolongated weight functions:

$$\widetilde{f}_{j,m,k}^{(\ell)}(\sigma_0) = f_{m,k}(\sigma_0)\,\frac{\widehat{\phi}_{j,k}^{(\ell)}}{\widehat{f}_{m,k}(\sigma_0)}\,. \tag{10}$$

The fine group cross sections are then re-condensed to the coarse group structure with the scaled weight functions $\left(\widetilde{f}_{j,m,k}^{(\ell)}(\sigma_0)\right)$ and once more combined with the Bondarenko method. These iteration-dependent coarse group cross sections $\left(\Sigma_{j,g}^{(\ell)}\right)$ are used in the next outer iteration. This process is repeated until a desired convergence is reached.

In this work, the fine group cross sections are re-collapsed after every outer iteration. However, this group collapse could be performed every few iterations, which would decrease the additional time spent re-collapsing the cross sections while potentially changing the total number of iterations. We chose to repeat the group collapse every iteration to ensure the accuracy of the solution.

By scaling the fine group weight functions from NJOY, we preserve the original multigroup resonance information while also including spatial effects. Rather than using multidimensional calculations to obtain a weight function (e.g., a lattice or a CENTRM calculation), we use fluxes obtained in the course of a transport iteration to add spatial information to 0-D weight functions. Although multidimensional calculations might produce more accurate multigroup cross sections, they are problem specific. If one changes the design of a reactor fuel assembly, for example, then new lattice calculations must be performed. With OTF weighting, only self-shielded 0-D spectrums are required.

While we chose to use the OTF prolongations to scale the weight functions from NJOY, this is far from the only option. This on-the-fly weighting method can be applied to any given set of fine group cross sections and weight functions. For instance, one could perform infinite medium calculations for each material with the fine group cross sections and scale the resulting fluxes. Alternately, one could first combine the fine group data with the Bondarenko method and collapse these cross sections with a weight function scaled by the OTF prolongations. We chose to scale the isotope-dependent fine group weight functions to better match the LANL cross section processing code NDI [17].

Four prolongation methods are presented here. Each prolongation method assumes that the continuous energy weight function or neutron density has an average slope that is linear in either speed (v) or energy (E) within a coarse group. The slope is obtained from the coarse group fluxes or neutron densities for the given coarse group (g) and its two neighbors ($g+1$, $g-1$). The first and last coarse groups use a flat slope.

It is important to mention that only the shape of the weight function within a coarse group matters during a group collapse. None of the methods below preserve the total flux in a coarse group, but they are not intended to. The OTF weight functions are only meant to provide a solution-dependent shape within a coarse group, and not to produce consistent fine group fluxes.

1. Piecewise Linear $N(v)$

To derive the first OTF prolongation, we begin by assuming the neutron density within a coarse group g may be represented by

$$\begin{aligned}\widetilde{N}(v) &= \frac{N_g + N_{g+1}}{2} \\ &\quad + \frac{\left(N_{g-1}+N_g\right)/2 - \left(N_g + N_{g+1}\right)/2}{\Delta v_g}\left(v - v_{g+1/2}\right) \\ &= \frac{N_g + N_{g+1}}{2} + \frac{N_{g-1} - N_{g+1}}{2\Delta v_g}\left(v - v_{g+1/2}\right)\,. \end{aligned}\tag{11}$$

Here Δv_g is the speed width of energy bin g, $v_{g+1/2}$ is the speed at the lower boundary of group g, and N_g is the *average* neutron density in group g, calculated by

$$N_g = \left\langle \frac{1}{v} \right\rangle_g \frac{\phi_g}{V_g}\,, \tag{12}$$

where

$$V_g = \int_{\Delta v_g} v^2 dv = \frac{1}{3}\left(v_{g-1/2}^3 - v_{g+1/2}^3\right)\,, \tag{13}$$

$$\left\langle \frac{1}{v} \right\rangle_g = \frac{\int_{\Delta v_g} \frac{1}{v}\phi(v)\,dv}{\phi_g}\,, \tag{14}$$

and $v_{g-1/2}$ is the speed of the upper boundary of group g.

To obtain the corresponding approximate fine group flux for group k ($\widetilde{\phi}_k$, $k \in g$), we integrate $v\widetilde{N}(v)$ over $\Delta v_k = \left[v_{k+1/2}, v_{k-1/2}\right]$:

$$\begin{aligned}\widetilde{\phi}_k &= \int_{\Delta v_k} v\widetilde{N}(v)\,v^2 dv \\ &= \left[\left(\frac{N_g + N_{g+1}}{2} - \frac{N_{g-1} - N_{g+1}}{2\Delta v_g} v_{g+1/2}\right)\frac{v_{k-1/2}^4 - v_{k+1/2}^4}{4} \right. \\ &\qquad \left. + \frac{N_{g-1} - N_{g+1}}{2\Delta v_g}\,\frac{v_{k-1/2}^5 - v_{k+1/2}^5}{5}\right]. \end{aligned}\tag{15}$$

$\widetilde{\phi}_k$ may now be used to scale the original fine group weight functions, as previously described.

There are two important things to note in Eq. (15). First, we chose to calculate the fine group flux ($\widetilde{\phi}_k$) rather than the fine group number density ($\widetilde{N}_k$) because group collapses are typically performed using scalar fluxes as weights to preserve reaction rates [1, 2]. However, because we are using a ratio of OTF prolongations to scale a fine group weight function, we are not necessarily limited to using $\widetilde{\phi}_k$.

Second, we do not bother normalizing $\widetilde{\phi}_k$ because the fine-to-coarse group collapse depends on the relative magnitude of the flux *within* a coarse group. In other words, as long as the fine group fluxes are properly normalized relative to each other within a single coarse group, we do not need to normalize them across the entire energy domain.

2. Piecewise Linear $\phi(v)$

For the second prolongation method, we assume the neutron flux, rather than the neutron density, is linear in v within a coarse group:

$$\widetilde{\phi}(v) = \frac{\widehat{\phi}_g + \widehat{\phi}_{g+1}}{2} + \frac{\widehat{\phi}_{g-1} - \widehat{\phi}_{g+1}}{2\Delta v_g}\left(v - v_{g+1/2}\right) , \qquad (16)$$

where

$$\widehat{\phi}_g = \frac{\phi_g}{V_g} \qquad (17)$$

is the *average* neutron flux in group g. An average neutron flux is necessary to avoid biasing the flux by the group bin width.

Integrating Eq. (16) over Δv_k yields

$$\widetilde{\phi}_k = \left(\frac{\widehat{\phi}_g + \widehat{\phi}_{g+1}}{2} - \frac{\widehat{\phi}_{g-1} - \widehat{\phi}_{g+1}}{2\Delta v_g} v_{g+1/2}\right)\frac{v_{k-1/2}^3 - v_{k+1/2}^3}{3} + \frac{\widehat{\phi}_{g-1} - \widehat{\phi}_{g+1}}{2\Delta v_g}\frac{v_{k-1/2}^4 - v_{k+1/2}^4}{4} . \qquad (18)$$

3. Piecewise Linear $N(E)$

Here and in the following section, we assume that the neutron density and neutron flux, respectively, are piecewise linear in energy, rather than speed.

Representing the neutron density within a coarse group g by a linear function of E, we have:

$$\widetilde{N}(E) = \frac{N_g + N_{g+1}}{2} + \frac{N_{g-1} - N_{g+1}}{2\Delta E_g}\left(E - E_{g+1/2}\right) . \qquad (19)$$

Here $E_{g+1/2}$ is the energy at the lower boundary of group g and N_g is again the average neutron density in group g, which is now calculated with the volume element of group g in energy-space, rather than speed-space:

$$V_g = \int_{\Delta E_g} dE = E_{g-1/2} - E_{g+1/2} = \Delta E_g . \qquad (20)$$

To obtain an estimate of the fine group flux, we integrate $v\widetilde{N}$ over $\Delta E_k = [E_{k+1/2}, E_{k-1/2}]$, yielding:

$$\widetilde{\phi}_k = \sqrt{\frac{2}{m}}\left[\left(N_g + N_{g+1} - \frac{N_{g-1} - N_{g+1}}{\Delta E_g} E_{g+1/2}\right)\frac{E_{k-1/2}^{3/2} - E_{k+1/2}^{3/2}}{3} + \frac{N_{g-1} - N_{g+1}}{\Delta E_g}\frac{E_{k-1/2}^{5/2} - E_{k+1/2}^{5/2}}{5}\right], \qquad (21)$$

where $E_{k+1/2}$ and $E_{k-1/2}$ are the lower and upper energy bounds of the fine group k, respectively, and $v = \sqrt{2E/m}$.

Eq. (21) is used in the same way as Eqs. (15) and (18). Because we are concerned only with ratios of prolongated fluxes, we neglect the $\sqrt{2/m}$ term.

4. Piecewise Linear $\phi(E)$

In our fourth method, we assume the neutron flux shape within a coarse group g may be represented by:

$$\widetilde{\phi}(E) = \frac{\widehat{\phi}_g + \widehat{\phi}_{g+1}}{2} + \frac{\widehat{\phi}_{g-1} - \widehat{\phi}_{g+1}}{2\Delta E_g}\left(E - E_{g+1/2}\right) , \qquad (22)$$

where $\widehat{\phi}_g$ is defined in Eq. (17).

Integrating over a fine group ΔE_k, we obtain

$$\widetilde{\phi}_k = \left[\frac{\widehat{\phi}_g + \widehat{\phi}_{g+1}}{2} - \frac{\widehat{\phi}_{g-1} - \widehat{\phi}_{g+1}}{2\Delta E_g} E_{g+1/2}\right]\Delta E_k + \frac{\widehat{\phi}_{g-1} - \widehat{\phi}_{g+1}}{2\Delta E_g}\frac{E_{k-1/2}^2 - E_{k+1/2}^2}{2} , \qquad (23)$$

our final OTF prolongation.

5. Other variations

There are many other potential prolongation methods. In the above four we assumed the neutron density and flux were piecewise linear functions of either speed or energy. We could have, for instance, used a spline interpolation or an expansion in energy squared. The choice of a piecewise linear in speed neutron density was based on a similar approximation in PARTISN for moving material momentum advection corrections [18]. The other three prolongations were natural extensions of this one.

As shall be shown in the following section, the choice of prolongation is frequently less important than having some prolongation to adjust cross sections on-the-fly.

V. TESTING

The OTF weighting method was tested with five problems: (1) a 1-D uranium oxide (UO_2) slab; (2) a 1-D slab of mixed-oxide (MOX), water, and UO_2; (3) a 1-D slab of Pu/U metal, liquid sodium, and UO_2; (4) a 2-D Cartesian problem with UO_2 and water; and (5) a 2-D Cartesian problem with Pu/U and sodium. Their isotopics are presented in Table I. The geometries for the 1-D problems are also given in Table I, while the geometry and boundary conditions for the 2-D problems are shown in Figure 2. The UO_2 slab has a vacuum boundary condition on the right and a reflecting boundary condition on the left, while the MOX-water-UO_2 (MWU) and plutonium/uranium-sodium-UO_2 (PuNaU) problems have reflecting boundary conditions on both sides.

1. Test Problem Flux Comparison

Figure 3 compares the calculated 618 group PARTISN scalar fluxes integrated over the entire geometry for each problem to the infinitely dilute TD-4 weight function. It is important to again note that differences in weight functions are only important *within* a coarse group. Even if their magnitudes are dissimilar, two different weight functions can still lead to similar coarse group cross sections. In Figure 3 the ordinate axis is the multigroup flux divided by lethargy bin width (Δu).

TABLE I: Problem Definitions

Problem	Region	Length (cm) or Area (cm^2)	Isotope 1	Number Density	Isotope 2	Number Density	Isotope 3	Number Density
UO_2 Slab	1	20 cm	U-235	0.00320772	U-238	0.021265613	O-16	0.0489467
MWU Slab	1	0.1837237 cm	Pu-239	0.00124814	U-238	0.023225193	O-16	0.0489467
	2	1 cm	H-1	0.05008667	O-16	0.025043333		
	3	0.5505 cm	U-235	0.00124814	U-238	0.023225193	O-16	0.0489467
PuNaU Slab	1	0.125 cm	Pu-239	0.002527705	U-238	0.02137352		
	2	0.625 cm	Na-23	0.0121410395				
	3	0.25 cm	U-235	0.002139046	U-238	0.008665411	O-16	0.0145637
UO_2 2-D	1	281.25 cm^2	U-235	0.00457455	U-238	0.0182982	O-16	0.0457642
	2	618.75 cm^2	H-1	0.0496224	O-16	0.0248112	B-10	0.0000107
Pu 2-D	1	281.25 cm^2	Pu-239	0.0120793761	U-238	0.0362381282		
	2	618.75 cm^2	Na-23	0.01214104				

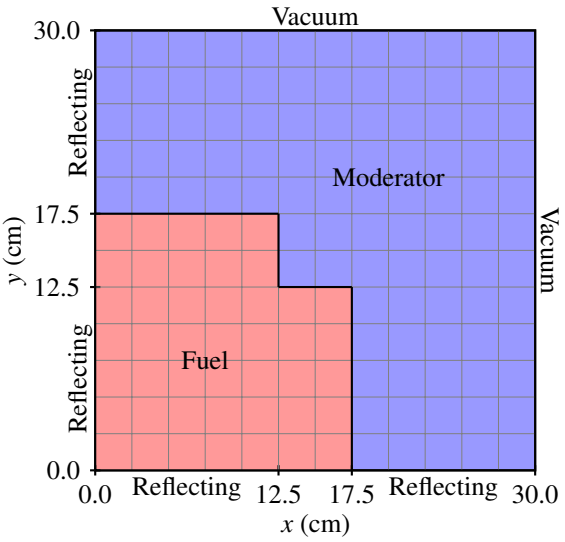

Fig. 2: 2-D Geometry

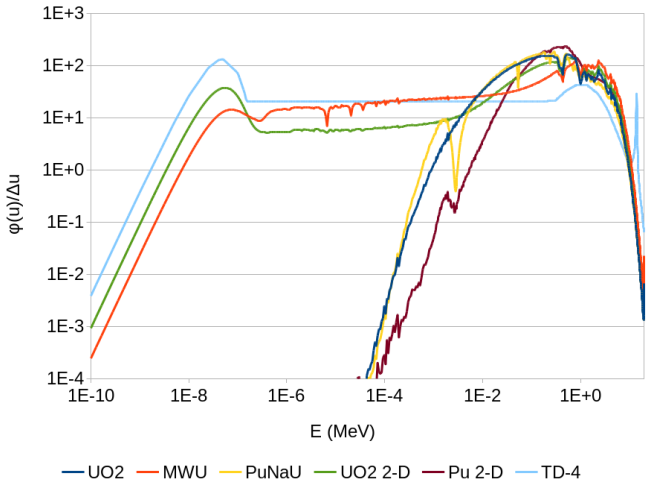

Fig. 3: Weight function comparison

Unsurprisingly, the two problems with water, MWU and UO_2 2-D, have thermal spectrums, while the other three have fast spectrums. The Pu 2-D problem has the fastest spectrum because it has a poor moderator (sodium) and vacuum boundary conditions, which allow neutrons to escape before they can thermalize. While the UO_2 slab also has vacuum boundary conditions, the problem is sufficiently large that neutron leakage is less significant. Likewise, the PuNaU slab, which has the same moderator as the Pu 2-D problem, has a spectrum comparable to the UO_2 slab because there is no leakage.

Many of the resonances at higher energies (400 keV to 10 MeV) come from O-16. The dip at 2.8 keV seen in the PuNaU and Pu 2-D problems come from a sharp Na-23 resonance, as does the dip at 53 keV. Between 1 eV and 20 keV, we see the effects of the uranium and plutonium resonances. They are likely less evident in the 2-D problem because the integration over the entire geometry includes more moderator than with the PWU slab. The shoulder at 4 MeV seen in most of the spectrums is from the elastic scattering cross section for the actinides.

2. Test Problem Results

Reaction rates (RR) and eigenvalues were obtained for each problem, collapsing method, and coarse group structure in order to evaluate the accuracy of OTF weight functions. Both removal (taken as (n,2n) + (n,3n) + (n,γ) + (n,α) + (n,p) + (n,d) + (n,t) + (n,f)) and fission reaction rates are compared. MCNP results are presented for further comparisons. For the 2-D problems, fission source errors relative to the 618 group solution are shown for each 30 group solution as a function of space.

The OTF weight functions typically improved the coarse group PARTISN solution over the standard group collapse method when compared to the 618 group PARTISN solution, though this improvement varied. The eigenvalue error was reduced for every problem except the 30 group MWU slab and the UO_2 2-D 133 group solution. Likewise, the reaction rate errors decreased for all but the MWU and PuNaU problems. In those two problems, the OTF weighting methods struggled to capture the removal rate in the moderator.

TABLE II: UO_2 Slab

			Removal				Fission			
		k	Center	Middle	Edge	Sum	Center	Middle	Edge	Sum
MCNP		0.95188	0.00329	0.00256	0.00125	0.00710	0.00172	0.00134	0.00066	0.00372
618		0.95268	0.00335	0.00249	0.00127	0.00711	0.00175	0.00131	0.00067	0.00372
		Δk	ΔRR	(% Error)						
30	Standard	-0.011181	-0.403%	-0.454%	-0.579%	-0.452%	-1.135%	-1.157%	-1.176%	-1.150%
	PL $N(v)$	-0.004367	-0.094%	-0.099%	-0.123%	-0.101%	-0.443%	-0.435%	-0.412%	-0.435%
	PL $\phi(v)$	-0.003404	-0.056%	-0.054%	-0.064%	-0.057%	-0.345%	-0.334%	-0.307%	-0.334%
	PL $N(E)$	-0.003992	-0.101%	-0.102%	-0.114%	-0.104%	-0.408%	-0.398%	-0.368%	-0.397%
	PL $\phi(E)$	-0.003137	-0.092%	-0.087%	-0.082%	-0.088%	-0.323%	-0.310%	-0.273%	-0.310%
133	Standard	-0.001496	-0.088%	-0.085%	-0.074%	-0.084%	-0.162%	-0.156%	-0.132%	-0.155%
	PL $N(v)$	-0.000553	-0.050%	-0.039%	-0.009%	-0.039%	-0.068%	-0.057%	-0.024%	-0.056%
	PL $\phi(E)$	-0.000539	-0.051%	-0.041%	-0.010%	-0.040%	-0.067%	-0.056%	-0.022%	-0.055%
250	Standard	-0.000451	-0.027%	-0.026%	-0.020%	-0.025%	-0.050%	-0.048%	-0.038%	-0.047%
	PL $\phi(E)$	-0.000153	-0.017%	-0.014%	-0.003%	-0.013%	-0.020%	-0.017%	-0.005%	-0.016%

In all five problems, the OTF results varied little between prolongations for 133 and 250 groups. Therefore, only selected results are presented.

In Tables II – VI, eigenvalue errors are presented as the difference between the 618 group PARTISN solution and the coarse group solutions:

$$\Delta k = k_{PARTISN,\ Fine} - k_{PARTISN,\ Coarse}\ , \tag{24}$$

while reaction rate errors are given as percent errors:

$$\Delta\text{RR} = \frac{\text{RR}_{PARTISN,\ Fine} - \text{RR}_{PARTISN,\ Coarse}}{\text{RR}_{PARTISN,\ Fine}} \times 100\%\ . \tag{25}$$

Reaction rates were normalized to neutron production such that for each solution

$$\frac{1}{k}\int_V \sum_{g=1}^{G} \nu\Sigma_{f,g}\phi_g dV = 1\ . \tag{26}$$

A. UO_2 Slab Results

Eigenvalue and reaction rate results for this simple problem are presented in Table II. The slab is split into three equal length regions for reporting reaction rates – the center, middle, and edge. The size of this problem, along with oxygen acting as the primary moderator, yielded a spectrum (see Figure 3) almost as fast as the Pu 2-D problem.

In every case, OTF weighting improved the eigenvalue and the integral reaction rates. However, the errors for each coarse group structure were slight even with the standard group collapse (less than 1.2%), particularly for 133 and 250 energy groups. Therefore, only the relative improvement (comparing the OTF errors to the standard collapsing method errors) is significant. For example, the 30 group standard removal rate error for the central region is -0.403%. With PL $N(v)$, the error is -0.094%. Thus, while the absolute improvement is only 0.309%, the relative improvement is greater than a factor of four.

The reduction in both eigenvalue and reaction rate error is comparable for all four OTF weight functions. The relative improvement in reaction rates increases towards the boundary of the problem, where the vacuum boundary condition has a greater impact on the spectrum. With 30 groups, we see a common trend – while the prolongation with the most accurate eigenvalue has the most accurate fission rates, another prolongation more accurately captures the removal rates. A comparison of the fission rate errors as a function of space showed little variation between the methods (variations of up to 0.06%).

B. MOX-Water-UO_2 Slab Results

The MOX-Water-UO_2 (MWU) slab, with results shown in Table III, is the second-most thermal problem tested. Therefore, epithermal resonances, such as those seen in U-235, U-238, and Pu-239, have a significant impact on the final solution. This is the only problem where, for 30 groups, the OTF methods yielded a less accurate eigenvalue than the standard group collapse. It is also one of two problems where, for 30 groups, the most accurate eigenvalue does not correspond to the most accurate fission reaction rates.

While the OTF methods generally show improvement in the reaction rate errors over the standard group collapse, these improvements are slight. Furthermore, the OTF methods performed worse in the moderator region than the standard group collapses. These inaccuracies are likely responsible for the increased 30 group eigenvalue error: as the removal reaction rate error in the water increases, so does the eigenvalue error. Additionally, the reaction rate errors are lopsided – both removal and fission rates were underestimated in the MOX and overestimated in the UO_2.

Again, these errors are small compared to the 618 group solution, on the order of 2.5% or less. Variations between the methods thus led to no more than a 0.5% change in the relative error. When comparing the fission rate as a function of space, errors are as large as 6%. While OTF weighting improved this

TABLE III: MOX-Water-UO_2 Slab

			Removal			Fission		
		k	MOX	Water	UO_2	MOX	Water	UO_2
MCNP		1.44474	0.003915	0.000225	0.005903	0.002133	0.000000	0.003398
618		1.44957	0.003916	0.000222	0.005902	0.002141	0.000000	0.003408
		Δk	ΔRR	(% Error)				
30	Standard	0.003213	2.110%	2.011%	-1.538%	1.583%	0.000%	-0.777%
	PL $N(v)$	0.003491	2.028%	2.183%	-1.470%	1.514%	0.000%	-0.689%
	PL $\phi(v)$	0.003727	1.869%	2.349%	-1.369%	1.355%	0.000%	-0.545%
	PL $N(E)$	0.003711	1.961%	2.257%	-1.427%	1.453%	0.000%	-0.619%
	PL $\phi(E)$	0.004193	1.761%	2.535%	-1.303%	1.268%	0.000%	-0.426%
133	Standard	0.002395	0.928%	0.052%	-0.622%	0.718%	0.000%	-0.240%
	PL $N(v)$	0.001055	0.620%	-0.072%	-0.410%	0.364%	0.000%	-0.140%
	PL $\phi(E)$	0.001470	0.626%	-0.000%	-0.417%	0.383%	0.000%	-0.105%
250	Standard	0.000504	0.486%	-0.113%	-0.320%	0.421%	0.000%	-0.249%
	PL $\phi(E)$	-0.000296	0.251%	-0.120%	-0.163%	0.187%	0.000%	-0.174%

TABLE IV: PuNaU Slab

			Removal			Fission		
		k	Pu/U	Na	UO_2	Pu/U	Na	UO_2
MCNP		1.43169	0.004443	0.000030	0.005602	0.002151	0.000000	0.003251
618		1.43890	0.004420	0.000025	0.005627	0.002160	0.000000	0.003271
		Δk	ΔRR	(% Error)				
30	Standard	-0.014246	0.124%	1.116%	-0.176%	-0.915%	0.000%	-0.968%
	PL $N(v)$	-0.009105	0.002%	2.603%	-0.112%	-0.602%	0.000%	-0.611%
	PL $\phi(v)$	-0.007963	-0.035%	2.053%	-0.071%	-0.554%	0.000%	-0.512%
	PL $N(E)$	-0.008314	-0.015%	2.173%	-0.095%	-0.552%	0.000%	-0.556%
	PL $\phi(E)$	-0.006796	-0.045%	1.428%	-0.057%	-0.461%	0.000%	-0.446%
133	Standard	-0.002782	0.057%	0.492%	-0.033%	-0.204%	0.000%	-0.177%
	PL $\phi(E)$	-0.001151	0.008%	1.566%	0.005%	-0.113%	0.000%	-0.052%
250	Standard	-0.000880	0.034%	0.930%	-0.013%	-0.066%	0.000%	-0.055%
	PL $\phi(E)$	-0.000536	0.013%	0.865%	-0.003%	-0.051%	0.000%	-0.026%

error, the improvement is small.

C. PuNaU Slab Results

The Pu/U-Na-UO_2 (PuNaU) slab has a spectrum comparable to the UO_2 slab, though with significant dips due to Na-23 resonances. Table IV shows the eigenvalue and reaction rate errors for this problem. Once more, the OTF methods yielded less accurate solutions (compared to the standard group-collapse) in the moderator for 30 and 133 groups while producing more accurate solutions in the fuel regions. Eigenvalue errors were decreased by up to a factor of two, and reaction rate errors (when improved) were similarly decreased.

The spatial fission rate distribution once more showed minimal variation between the methods (variations of up to 0.04%), similar to the UO_2 problem. This, however, masks the flux error in the sodium revealed by the reaction rates.

D. UO2 2-D Slab Results

Reaction rates and eigenvalues are given in Table V for this large, thermal, 2-D problem. The OTF weighting methods yielded significantly lower reaction rate errors for the 30 group solutions (on average, the errors were reduced by more than 50%). The difference in these errors decreases as the number of energy groups increases until, with 250 energy groups, the OTF removal reaction rates are less accurate than the standard collapsing method. Eigenvalue errors are also inconsistent, with the OTF methods performing worse than the standard method for 133 groups, likely due to cancellation of errors (the standard 133 group eigenvalue is more accurate than even the 250 group solution).

Figures 4a – 4e show the fission rate error (based on the 618 group solution) as a function of space for the five 30 group solutions, with the problem split into 5 cm by 5 cm regions for reporting the fission rates. The OTF weighting methods reduced the root-mean-square (RMS) error by more than a factor of two. Again we see little deviation between the OTF

TABLE V: UO_2 2-D

			Removal		Fission
		k	Fuel	Water	Fuel
MCNP		0.95380	106182.46	54604.20	69550.55
618	Standard	0.95561	106246.84	54147.26	69686.24
		Δk	ΔRR	(% Error)	
30	Standard	-0.001491	-0.571%	0.751%	-0.119%
	PL $N(v)$	0.000346	-0.191%	-0.076%	0.063%
	PL $\phi(v)$	0.000587	-0.134%	-0.196%	0.087%
	PL $N(E)$	0.000377	-0.185%	-0.105%	0.065%
	PL $\phi(E)$	0.000567	-0.157%	-0.183%	0.065%
133	Standard	0.000007	-0.088%	0.086%	0.007%
	PL $N(v)$	0.000030	-0.034%	-0.006%	0.007%
	PL $\phi(E)$	0.000025	-0.038%	0.005%	0.006%
250	Standard	0.000143	-0.003%	-0.069%	0.017%
	PL $N(v)$	0.000002	0.015%	-0.087%	0.001%
	PL $\phi(E)$	-0.000014	0.013%	-0.077%	-0.001%

TABLE VI: Pu 2-D

			Removal		Fission
		k	Pu/U	Na	Pu/U
MCNP		1.05206	182167.00	46.00	108327.31
618	Standard	1.05196	182204.82	44.57	108318.36
		Δk	ΔRR	(% Error)	
30	Standard	0.003704	-0.746%	-2.840%	0.372%
	PL $N(v)$	0.000708	-0.043%	-0.237%	0.095%
	PL $\phi(v)$	0.000436	-0.029%	-0.161%	0.065%
	PL $N(E)$	0.000742	-0.070%	-0.121%	0.094%
	PL $\phi(E)$	0.000722	-0.097%	-0.120%	0.088%
133	Standard	0.000587	-0.086%	-1.457%	0.058%
	PL $\phi(E)$	0.000065	-0.009%	-0.357%	0.006%
250	Standard	0.000205	-0.029%	0.008%	0.020%
	PL $N(v)$	-0.000006	-0.004%	-0.178%	-0.001%
	PL $\phi(E)$	-0.000009	-0.004%	-0.164%	-0.001%

methods. By RMS error, $\phi(v)$ produced the most accurate results while $N(v)$ yielded the least. The integral fission rates, however, show the opposite. This reinforces that one must be careful when comparing integral reaction rates.

E. Pu 2-D Slab Results

Table VI presents results for the Pu 2-D problem, which has the fastest spectrum of the five test problems. Here, the OTF methods yielded more accurate eigenvalues and reaction rates, even in the moderator. The only exception was the 250 group removal rate in the sodium. Eigenvalue errors decreased by a factor of five or more, while reaction rate errors were improved by a factor of four or more. Once more, there is no consistently "best" OTF method: for 30 groups, $\phi(v)$ is the most accurate; for 133 groups, $\phi(E)$; for 250 groups, arguably either $N(v)$ or $\phi(E)$.

Figures 5a – 5e show the fission rate error (based on the 618 group solution) as a function of space for the five 30 group solutions. Here the improvement with OTF weight functions is clearly evident when compared to the standard collapsing method. The OTF weight functions decrease the RMS error by anywhere from a factor of four to a factor of thirteen. $N(v)$ yielded the best results by RMS error, while $\phi(E)$ yielded the worst. However, by the integral fission rate, $\phi(v)$ is the most accurate (see Table VI). Again, integral reaction rates should be viewed with caution, as they are more easily affected by cancellation of error.

3. Test Problem Summary

In general, the OTF methods improved the coarse group solutions for each test problem. This improvement was far from consistent; for the MWU, PuNaU, UO_2 2-D, and Pu 2-D problems, the OTF weight functions occasionally yielded

less accurate solutions than the standard weight function. For the two slabs (both reflecting), the OTF methods struggled to capture the removal reaction rate in the moderator regions, where the removal rates are small. The UO_2 2-D and Pu 2-D problems both led to inaccurate 250 group removal rates – for UO_2 in both the fuel and moderator; for Pu only in the moderator. For the 30 group MWU slab and the 133 group UO_2 2-D problems the OTF solutions showed an increase in eigenvalue error. For the former, the errors correspond to errors in the moderator. For the latter, this increase likely comes from cancellation of error.

Despite these less accurate examples, the OTF weight functions have shown that, given a set of fine group cross sections, they can produce coarse group solutions that are frequently closer to the fine group solution than with the standard group collapse. While this improvement was slight in some cases, such as the MWU and PuNaU reflecting slabs, OTF weight functions, on average, reduced eigenvalue errors by more than 200%, and reaction rate errors by more than 300%. OTF weighting appears to do better in problems with fewer resonances. It performed the best with the Pu 2-D test problem, which has the fewest resonances (see Figure 3), and the worst with the MWU slab, which had the most resonances, particularly in the epithermal range. However, while the OTF methods may improve eigenvalues and reaction rates relative to the fine group solution, they will not necessarily make the solution more accurate compared to MCNP. As with the standard group collapse, we can only expect the coarse group solution to do as well as the fine group solution.

The differences between the four OTF methods were inconsistent from problem to problem. Occasionally, one of the four prolongations would yield the most accurate k, while another would produce more accurate reaction rates. Despite these inconsistencies, PL $\phi(E)$ was most frequently the most accurate prolongation, followed by PL $N(v)$.

The eigenvalue errors typically mirrored the fission reaction rates at the expense of the removal rates. In other words, the case with the most accurate eigenvalue frequently had the most accurate fission reaction rates, while another case would have the more accurate removal rates. Because k is primarily determined by the fission rate, an accurate eigenvalue only requires the flux to be accurate where $\nu\Sigma_f$ is large. This does not guarantee that the flux will be accurate at other energies, where other cross sections may dominate.

Because group collapses are performed with $\phi(E)$, one might assume that piecewise linear in $\phi(E)$ would be the most accurate method. Each of the four OTF prolongations is, in essence, a polynomial expansion of E within in a group. As such, there is no reason to expect a linear expansion in E (as with the $\phi(E)$ OTF prolongation) to do better than the three other prolongations.

VI. CONCLUSIONS

In this paper, we have presented a new method for collapsing fine group cross sections on-the-fly that relies solely on the previous iteration's coarse group fluxes and the information from NJOY. With OTF weight functions, we saw significant decreases in the eigenvalue errors for the coarse group solutions, particularly in the 2-D problems. Only in a few cases (the MWU 30 group cases and UO_2 2-D 133 group cases) did the OTF prolongations yield a less accurate eigenvalue than the standard weight functions. Reaction rate errors, while less consistent than the eigenvalues, were nevertheless frequently improved with the OTF weight functions, often by more than a factor of three. Only in moderator regions in the reflecting 1-D slabs and the 250 group 2-D problems, as well the fuel region for the 250 group UO_2 2-D case, did we see increases in removal reaction rate errors.

The piecewise linear $\phi(E)$ weight function often proved the most accurate, though all four prolongations improved the solution. This implies that the choice of which OTF weight function method is less important than having *an* OTF weight function. In other words, introducing information from the problem of interest yielded better results than a traditional static group collapse, as expected. Furthermore, as the number of energy groups increased, the differences between the four methods decreased considerably. As the width of each coarse group decreases, variations in a group are likely to be smaller, which decreases the impact of the weight function method.

Our results ultimately show that with OTF weight functions one can run a coarser group structure and obtain results close to the fine group solution, thus increasing the speed of a calculation without significantly compromising accuracy. We have not yet investigated the increased run time with OTF weighting because it has not yet been optimized. Although not shown, OTF weighting had a minimal impact on the number of inner iterations (within-group scattering sweeps) when compared to the standard condensation method. While OTF weighting occasionally decreased the number of outer iterations, the total number of inner iterations varied by no more than 15%. When OTF did increase the total number of iterations, it did so by no more than 3%.

While other re-condensation schemes exist, ours is unique in requiring neither an additional fine group transport solution nor additional coarse group equations. Furthermore, because we have no additional transport equations, there is no additional impact for time-dependent calculations (e.g., increased storage). For instance, a time-dependent SGD calculation would require a fine group time-derivative, which would require storage of the fine group angular fluxes from iteration to iteration. The OTF re-condensation scheme presented here may also be more parallelizable than the other methods. With spatial domain decomposition, the re-collapse can be performed separately on each coarse mesh, minimizing communication.

More tests, particularly ones that are more heterogeneous or 3-D, are required before categorically stating whether or not OTF weighting is superior to the standard weighting methods. The initial results presented here indicate that OTF weighting performs better when resonances are less significant. Once we have further investigated the applicability of OTF weighting to a range of problems, we will study the applicability of OTF weighting to time-dependent problems.

The OTF method can be easily modified to apply to time-dependent problems. In addition to the steps in the OTF weighting flow chart, one would only need to recalculate σ_0 as the material compositions changed with time. Furthermore,

rather than re-collapsing the cross sections after an outer iteration, one could collapse the fine group cross sections only at the beginning of time step using the previous time's flux solution, reducing the total time spent re-collapsing cross sections.

VII. ACKNOWLEDGMENTS

Los Alamos National Laboratory is operated by Los Alamos National Security, LLC, for the United States Department of Energy under Contract no. DE-AC52-06NA25396. LA-UR-17-21243.

REFERENCES

1. A. HEBERT, *Applied Reactor Physics*, Presses Internationales Polytechnique (2009).
2. E. E. LEWIS and W. F. MILLER, *Computational Methods of Neutron Transport*, American Nuclear Society, La Grange Park, Il, USA (1993).
3. I. I. BONDARENKO, "Group Constants for Nuclear Reactor Calculations," Consultants Bureau, New York (1964).
4. M. C. WHITE, "The TD Weight Function Revisited," LANL (2005), Internal Memo, X-5:MCW-05-24(U).
5. M. C. WHITE, "The 618-, 250-, 133-, and 70-Group LANL Neutron Energy-Group Structures," Los Alamos National Laboratory (2005), Internal Memo, X-5:MCW-05-94.
6. S. DOUGLASS, F. RAHNEMA, and B. FORGET, "Generalized Energy Condensation Theory," *Nuclear Science and Engineering*, **160**, pp. 41–58 (2008).
7. S. DOUGLASS and F. RAHNEMA, "Cross Section Recondensation Method via Generalized Energy Condensation Theory," *Annals of Nuclear Energy*, **38**, pp. 2105–2110 (2011).
8. S. DOUGLASS and F. RAHNEMA, "Consistent Generalized Energy Condensation Theory," *Annals of Nuclear Energy*, **48**, pp. 84–101 (2012).
9. L. ZHU and B. FORGET, "A Discrete Generalized Multigroup Energy Expansion Theory," *Nuclear Science and Engineering*, **166**, pp. 239–253 (2010).
10. L. ZHU, *Discrete Generalized Multigroup Theory and Applications*, Ph.D. thesis, Massachusetts Institute of Technology (November 2011).
11. S. DOUGLASS and F. RAHNEMA, "Subgroup Decomposition Method," *Annals of Nuclear Energy*, **48**, pp. 84–101 (2012).
12. "SCALE Code System," ORNL/TM-2005/39, Version 6.2, Oak Ridge National Laboratory, Oak Ridge, TN (2016). Los Alamos National Laboratory, LA-UR-12-27079 (2012).
13. D. W. MUIR, R. M. BOICOURT, and A. C. KAHLER, "The NJOY Nuclear Data Processing System, Version 2012," Los Alamos National Laboratory, LA-UR-12-27079 (2012).
14. J. R. ASKEW, F. J. FAYERS, and P. B. KEMSHELL, "A General Description of the Lattice CODE WIMS," *J. British Nucl. Energy Soc.*, **5**, pp. 564–585 (1966).
15. *MPACT Theory Manual Version 2.0.0*, March 11 (2015).
16. M. SEGEV, "Interpolation of Resonance Integrals," *Nucl. Sci. Eng.*, **79**, pp. 133–118 (1981).
17. M. G. GRAY, "NDI 2.0 Conceptual Design," LANL (2003), Internal Memo, CCN-12:03-17(U).
18. E. D. FICHTL, R. S. BAKER, and J. A. DAHL, "A Surface Integral Based Momentum Advection Scheme for Neutron Transport in Moving Materials," in "Joint International Conference on Mathematics and Computation (M&C), Supercomputing in Nuclear Applications (SNA), and the Monte Carlo (MC) Method," (April 2015).

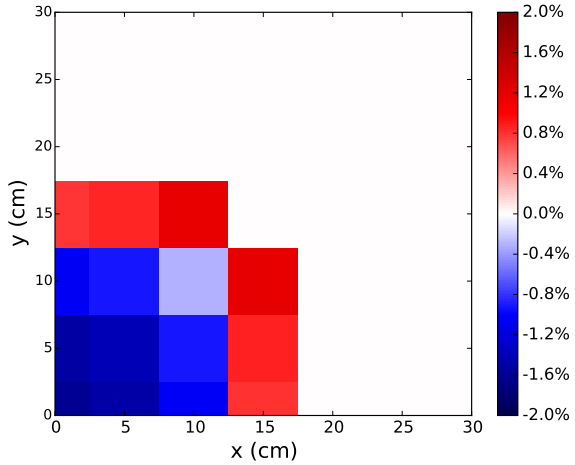

(a) Standard, RMS Error = 1.076 %

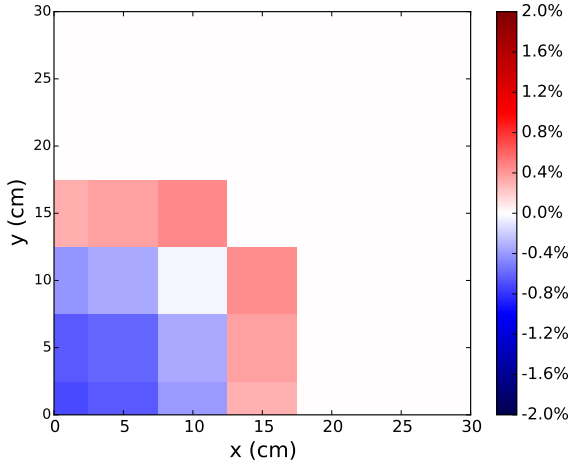

(b) $N(v)$, RMS Error = 0.443 %

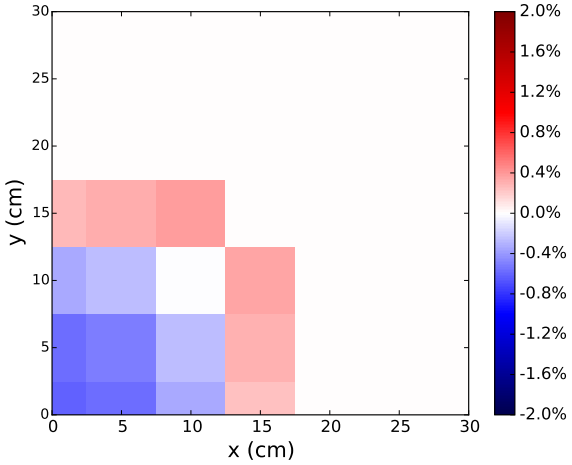

(c) $\phi(v)$, RMS Error = 0.373 %

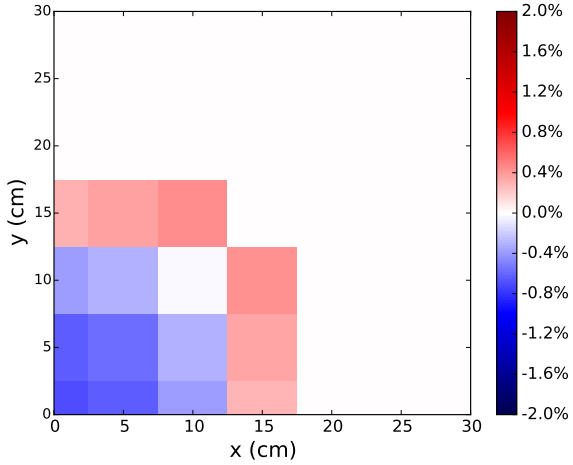

(d) $N(E)$, RMS Error = 0.427 %

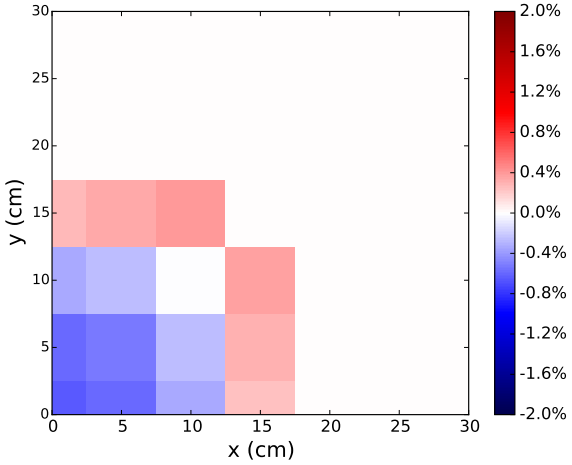

(e) $\phi(E)$, RMS Error = 0.387 %

Fig. 4: UO_2 Fission Rate Spatial Errors

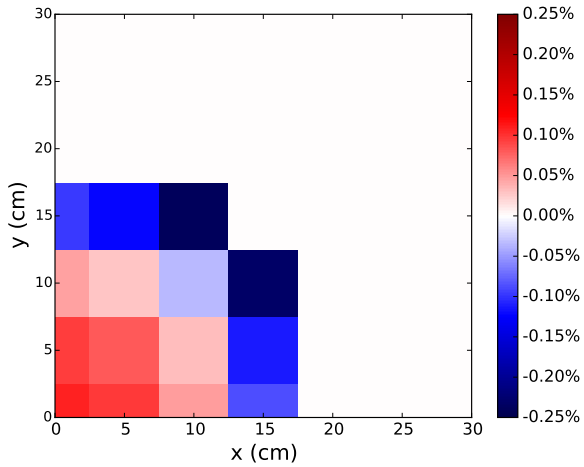

(a) Standard, RMS Error = 0.112 %

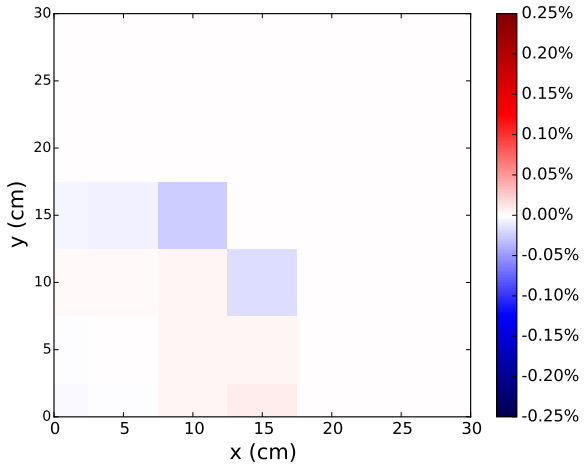

(b) $N(v)$, RMS Error = 0.008 %

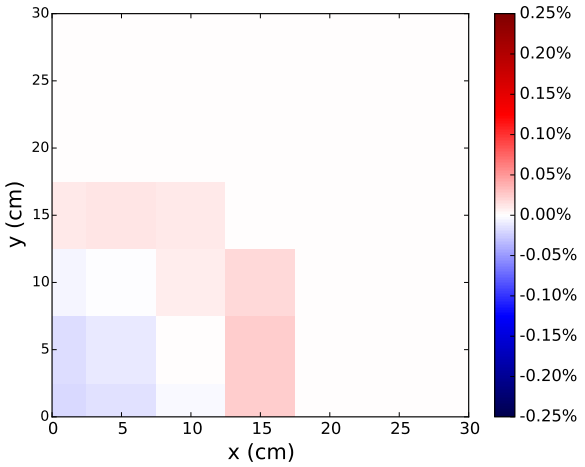

(c) $\phi(v)$, RMS Error = 0.014 %

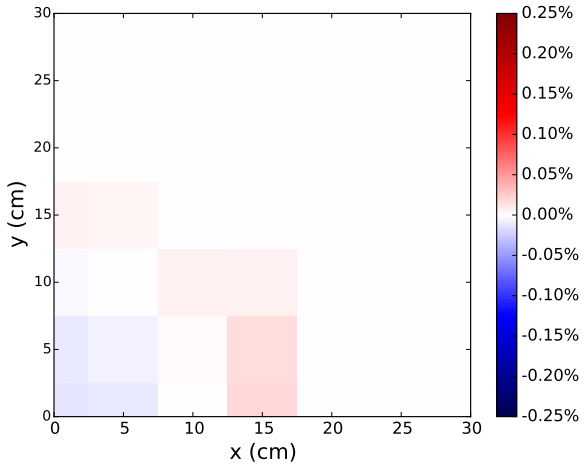

(d) $N(E)$, RMS Error =0.009 %

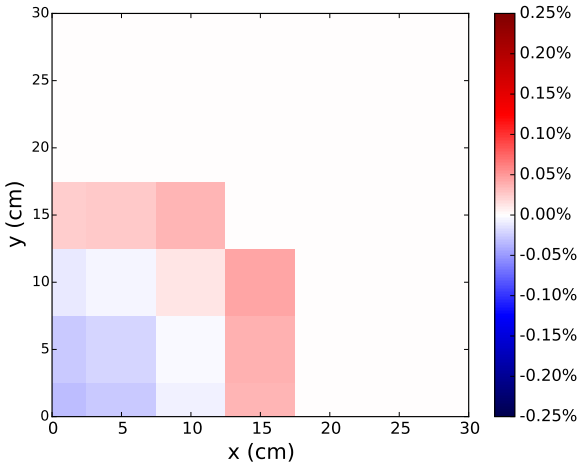

(e) $\phi(E)$, RMS Error = 0.025 %

Fig. 5: Pu Fission Rate Spatial Errors